Title
DIFFUSION FROM A LINE SOURCE IN A MAGNETIC FIELD

Authors
Berkner, Klaus H.
Pyle, Robert V.
Rugge, Henry F.
et al.

Publication Date
1963-06-23

UCRL-10801

University of California

Ernest O. Lawrence Radiation Laboratory

DIFFUSION FROM A LINE SOURCE IN A MAGNETIC FIELD

VI. International Conference on Ionization Phenomena in Gases - Paris, July 8-13, 1963

UCRL-10801

UNIVERSITY OF CALIFORNIA
Lawrence Radiation Laboratory
Berkeley, California

Contract No. W-7405-eng-48

DIFFUSION FROM A LINE SOURCE IN A MAGNETIC FIELD

Klaus H. Berkner, Robert V. Pyle, Henry F. Rugge,
J. Warren Stearns, and Joseph Winocur

June 20, 1963

DIFFUSION FROM A LINE SOURCE IN A MAGNETIC FIELD

Klaus H. Berkner, Robert V. Pyle, Henry F. Rugge,
J. Warren Stearns, and Joseph Winocur

Lawrence Radiation Laboratory and Department of Physics
University of California
Berkeley, California

June 20, 1963

ABSTRACT

Electron and ion temperatures and densities have been measured with Langmuir probes and by the absorption of optical radiation in a strontium-seeded argon plasma produced by a 10- to 40-A discharge from an oven with a hollow cathode into a 30-cm long, 20-cm diameter conducting cylinder with conducting end plates. Rubidium light at 4215 Å, coincident with a principal line of singly ionized Sr, was transmitted through the plasma, and the amplitude and line shape were measured with a scanning Fabry-Perot interferometer to obtain ion temperatures. The axial density variation was approximately cosinusoidal.

DIFFUSION FROM A LINE SOURCE IN A MAGNETIC FIELD

Klaus H. Berkner, Robert V. Pyle, Henry F. Rugge,
J. Warren Stearns, and Joseph Winocur

Lawrence Radiation Laboratory and Department of Physics
University of California
Berkeley, California

June 20, 1963

I. INTRODUCTION

The density distribution of a weakly ionized plasma diffusing along and across a magnetic field from a source along the axis of a conducting cylinder with conducting end plates can be written

$$n(r, z) = \cos \frac{\pi z}{L} \left[A I_0(r/q) + B K_0(r/q) \right], \tag{1}$$

where I_0 and K_0 are modified Bessel functions, L is the length of the cylinder, and[1]

$$q = \frac{L}{\pi \omega_i \tau_i} \left(\frac{T_i}{T_i + T_e} \right)^{1/2} \tag{2}$$

or[2,3]

$$q = \frac{L}{\pi \omega_i \tau_i} \; . \tag{3}$$

Expression (2) applies if the flow to the end walls is ambipolar, whereas expression (3) applies if the electron flow to the end walls is negligible. If the radius of the cylinder is large compared with q, then for $q \lesssim r < R$,

$$n = n_0 \, r^{-1/2} \, e^{-r/q} \cos \frac{\pi z}{L}$$

By inserting values of q obtained from either (2) or (3), the radial part of equation (4) has been compared with experimental density measurements and fair agreement has been observed for intermediate values of radius, provided that certain assumptions are made about parameters that are not accurately known. For example, the particle mean free paths are not well known nor are the ion temperatures easily determined. The situation is summarized in recent review articles by Hoh,[4] Golant,[5] and Boeschoten.[6] For roughly similar experiments, the assumed ion temperatures vary from 0.1 to 2 eV, and consequently the value of q to be inserted in eq. (2) can be expected to be uncertain by at least 4 to 5. Part of the present experiment is a measurement of the ion temperature for several discharge parameters, by using an optical technique. Rubidium light at 4215 Å is coincident with a principal line of singly ionized Sr. From measurements of absorption and line shape of a beam that has traversed a Sr^+ or Sr^+-seeded plasma, it is possible to infer average ion temperatures and density gradients.

We know of only one other attempt[7] to measure the density variations parallel to the axis for roughly similar conditions. Although it was not possible to make measurements close to the end plates in that case, the ion density appeared to be independent of z.

II. THE EXPERIMENT

The experimental arrangement is shown in fig. 1. The hollow-cathode discharge, typically 10 to 40 A and 3 mm in diameter, was at the axis of a 30-cm long, 20-cm diameter conducting cylinder with conducting end plates. Each end plate had a hole at the axis 2 cm in diameter through which the arc core passed; the cathode and anode each were normally 5 cm outside of the cylindrical equipotential chamber. An axial magnetic field of up to 4700 G could be applied. Langmuir probes were introduced radially at the median plane, and the axial density variation at various radii could be determined with an "L-shaped" probe which moved parallel to the axis, at the wall, and was bent through a right angle to reach toward the axis. The magnetic field coils at the median plane were separated by 5 cm; 20-cm-high windows outside of the coils made it possible to transmit a light beam along chords at various radii. Strontium ions could be injected either from the hollow cathode itself or by evaporating Sr metal on the axis of the discharge, but off the median plane.

The optical arrangement is shown in fig. 2. A scanning Fabry-Perot interferometer crossed with a monochromator was used to measure emission and absorption line widths. The absorption profile was obtained by transmitting a beam of 4215-Å Rb light along chords through the plasma, and measuring the absorption coefficient as a function of optical frequency. The lamp was modulated at 70 cps; the output of the monochromator was fed into a lock-in-amplifier phase-locked to the lamp at the modulation frequency. Thus any 4215-Å light emitted by the plasma appeared as random noise. By interrupting the arc at regular intervals while the 4215-Å line was being scanned, it was possible to obtain the absorption profile (fig. 3). Ion and neutral densities are sufficiently low so that collision and Stark broadening are small compared with Doppler broadening. Thus ion temperatures may be estimated from the absorption width. It was not possible to measure absorption at radii less than 2 cm, because of the intense Sr^+ emission from the arc core. An upper limit to the temperature at the core can be obtained by measuring the self-broadened emission line of Sr^+, or else one of the Ar^+ lines.

III. RESULTS

Examples of the probe results obtained with argon at $p = 2 \times 10^{-3}$ Torr, $B = 700$ G, and $I = 10$ A are given in figs. 4 and 5. Figure 4 gives probe measurements of the radial variations of electron temperature, ion density, and floating potential. Figure 5 shows the axial density variation at two radii. The electron temperature and floating potential were found to be independent of axial position. The space potential measurements (not shown) are similar to the floating potentials but larger by approximately (2 to 3)T_e. For the same parameters, the optical measurements give ion temperatures at the core of less than 1 eV (emission), and at $r = 5$ cm of 0.1 ± 0.1 eV (absorption).

Large amplitude oscillations in the 2- to 200-kc/sec frequency range are observed when the conducting end plates are not present; i.e., when there are radial and axial electric fields. In many cases these frequencies are found to be associated with asymmetric plasma distributions rotating about the axis of the discharge. These observations have been correlated with probe measurements where it was observed that the direction of rotation changed at a radius of a few cm, depending upon the magnetic field strength, and in agreement with the $\vec{E} \times \vec{B}$ directions obtained from the radial potential distribution. With the end plates present, no oscillations of significant amplitude are observed outside of the central hot core.

The 4215-Å Rb line absorption experiment, however, may show rotation of the plasma as a whole. At low pressures the peaks of the absorption profile shifted by as much as 50 millikaysers from the zero-field position when the direction of the magnetic field was reversed. The observations were made at distances of 2 to 7 cm from the axis. The shifts were small for the parameters of figs. 4 and 5.

When the Sr was introduced through the hollow cathode, the Sr^+ density in the diffusion chamber decreased very rapidly as the tip of the hollow cathode was moved away from the hole in the end plate, indicating that the ions have fairly large radial velocity components when they emerge from the cathode.

At neutral pressures less than 3×10^{-4} Torr, and with no gas introduced through the anode, the "Mode II" type of arc[8] was observed. The Sr^+ density, determined by optical absorption, fell off slowly with radius, considerable electric noise was present, and the absorption width was too large to permit an ion-temperature determination.

IV. DISCUSSION

The general features of the experimental results are in agreement with Simon's model. The axial density distribution is roughly cosinusoidal and symmetrical about the median plane at a pressure of 2×10^{-3} Torr. At 0.5×10^{-3} Torr the distribution is peaked toward the cathode side but symmetry can be restored by introducing gas into a hollow anode. As in neutral-particle diffusion calculations, the length L to be inserted in the $\cos(\pi z/L)$ term is not the actual length, 30 cm, but rather an extrapolated length $L+2\epsilon$, where $\epsilon \approx 3/4\ \lambda$ for this geometry. It is assumed that ions and electrons do not return from the walls. We make a rough estimate of ϵ, starting with the Ar^+-Ar cross-section measurements of Chanin and Biondi,[9] 1.4×10^{-14} cm^2 at 0.1 eV. This gives a mean free path $\lambda' = 1.2$ cm at 2×10^{-3} Torr. If we assume an approximately ambipolar field in the axial direction, the effective mean free path is $\lambda \approx \lambda'(1+T_e/T_i) \approx 1.2(1+0.4/0.1) = 6$ cm. Thus $\epsilon \approx 4$ cm. This value is used in fig. 5. The agreement is less good if the Zharinov or Tonks model is used, in which the axial diffusion is not ambipolar. In order to check the sensitivity of the distribution to the shape of the magnetic field, we took measurements with the field at the median plane approximately 10% larger and smaller than at the ends; no significant variations were observed.

An approximate fit to the radial density distribution can be obtained by using eq.(1) and a boundary condition n=0 at the wall (fig. 4). At intermediate radii the distribution is approximately exponential, and in this region the e-folding length is approximately inversely proportional to B and proportional to p, in agreement with other experiments. The measured Sr ion temperatures increase with increasing I (to 0.5 ± 0.2 eV at 40 A and 2×10^{-3} Torr) and decreasing p(to 0.45 ± 0.2 eV at $p = 5\times10^{-4}$ Torr and 10 A); they may also change with the discharge geometry. Accurate temperature measurements were impossible at higher magnetic fields due to Zeeman splitting. For the densities and temperatures in these experiments it is reasonable to assume that the Ar^+ and Sr^+ ions have nearly the same temperature; thus the Ar^+-ion cyclotron radius is given by $r_{bi} = (910/B)(T_{ev})^{1/2}$ cm. For the conditions appropriate to fig. 4, $T_i \lesssim 0.1$ eV, these ion cyclotron radii are of the order of one-tenth of the e-folding lengths obtained from the radial density distributions.

The raidal variation of ion density as determined from Langmuir-probe measurements can be integrated along chords for comparison with the integrated densities obtained from optical absorption as a function of radius. The two types of measurements show the same dependence on experimental parameters, but the probe densities fall off somewhat more rapidly with radius.

The diffusion coefficients obtained from experimental q values taken from the probe measurements are given in the table for the Simon model

$$D_{\perp i}(q)_S = D_i^0 \left(1 + \frac{T_e}{T_i}\right) \frac{\pi^2 q^2}{L^2} \qquad (5)$$

and for the Zharinov[2] or Tonks[3] (f = 0) model

$$D_{\perp i}(q)_{Z,T} = D_i^0 \frac{\pi^2 q^2}{L^2} \ . \qquad (6)$$

Here, $p = 2 \times 10^{-3}$ Torr, $T_i = 0.1$ eV, $T_e = 0.4$ eV, $\lambda = 1.2$ cm. The classically predicted value of the radial diffusion coefficient is $D_{\perp i} = D_i^0 (1 + \omega_i^2 \tau_i^2)^{-1}$ with $D_i^0 = 1/3\ \lambda_i v_i$. From the table we see that the radial diffusion coefficients deduced from the experiment are several times larger than would be predicted from the Simon theory, but in rather good agreement with Zharinov and Tonks. The measured floating potentials suggest that the latter theories should be appropriate. The axial density distribution appears to be in slightly better agreement with the Simon model. The experiment is being extended to larger values of L.

B (G)	r_{bi} (cm)	q_{exp} (cm)	$D_{\perp i}(q)_S$ (cm^2/sec)	$D_{\perp i}(q)_{Z,T}$ (cm^2/sec)	$D_{\perp i}$ (cm^2/sec)
700	0.40	4.0	2.4×10^4	4.8×10^3	2.8×10^3
3200	0.09	0.65	6.6×10^2	1.3×10^2	1.8×10^2

We wish to thank Dr. C. M. Van Atta for supporting this research. Dr. Joseph Lipson participated in the early optical measurements. Dr. Wulf B. Kunkel made useful comments about the mean free paths. Mr. Vincent J. Honey designed and built most of the electronics circuitry associated with the discharge.

REFERENCES

1. Albert Simon, in Proceedings of the Second United Nations International Conference on the Peaceful Uses of Atomic Energy (United Nations, Geneva, 1958) Vol. 32, p. 343.
2. A. V. Zharinov, J. Nucl. Energy P. C. 1, 267, 271 (1960).
3. Lewi Tonks, Phys. Fluids 3, 758 (1960).
4. F. C. Hoh, Rev. Mod. Phys. 34, 236 (1962).
5. V. E. Golant, Usp. Fiz. Nauk 79, 377 (1963).
6. F. Boeschoten and F. Schwirzke, Nucl. Fusion 2, 54 (1962).
7. Stephen D. Rothleder, Charged Particle Diffusion and Energy Transport in a Highly Ionized, Magnetically Confined Plasma (Ph. D. Thesis) Massachusetts Institute of Technology, 1962 (unpublished).
8. R. V. Neidigh and C. H. Weaver, in Proceedings of the Second United Nations International Conference on the Peaceful Uses of Atomic Energy (United Nations, Geneva, 1958) Vol. 31, p. 315.
9. L. M. Chanin and M. A. Biondi, Phys. Rev. 106, 473 (1957).

FIGURE CAPTIONS

Fig. 1. The plasma-chamber geometry. R. P. = radial probe; A. P. = axial probe; W = window; D. P. = diffusion pump; H. C. = hollow cathode and oven; A = hollow anode; (Sr) = alternate positions for introducing strontium.

Fig. 2. The optical arrangement.

Fig. 3. (a) An example of a transmitted 4215-Å line profile. The log of the ratio of the upper and lower envelope is the absorption coefficient. (b) Sr^+ absorption profile deduced from data shown in (a). After correcting for instrument width and Zeeman effect, an ion temperature of (0.1 ± 0.1) eV was obtained; $p = 2\times10^{-3}$ Torr, B = 700 G, $r_{min} = 2$ cm, I = 10 A. There were about 10^{11} Sr^+ ions along the optical path. (Near 4215 Å, 1 millikayser = 1.78×10^{-4} Å.)

Fig. 4. Radial probe measurements. $p = 2\times10^{-3}$ Torr, B = 700 G, I = 10 A. The lines through the T_e and ϕ_f points are drawn to guide the eye. The n_i curve is normalized at r = 3.4 cm, with $A/B = -1.21\times10^{-2}$ in eq. (1).

Fig. 5. Axial probe measurements; $p = 2\times10^{-3}$ Torr, B = 700 G, I = 10A. ●, 2 cm; 0, 5 cm.

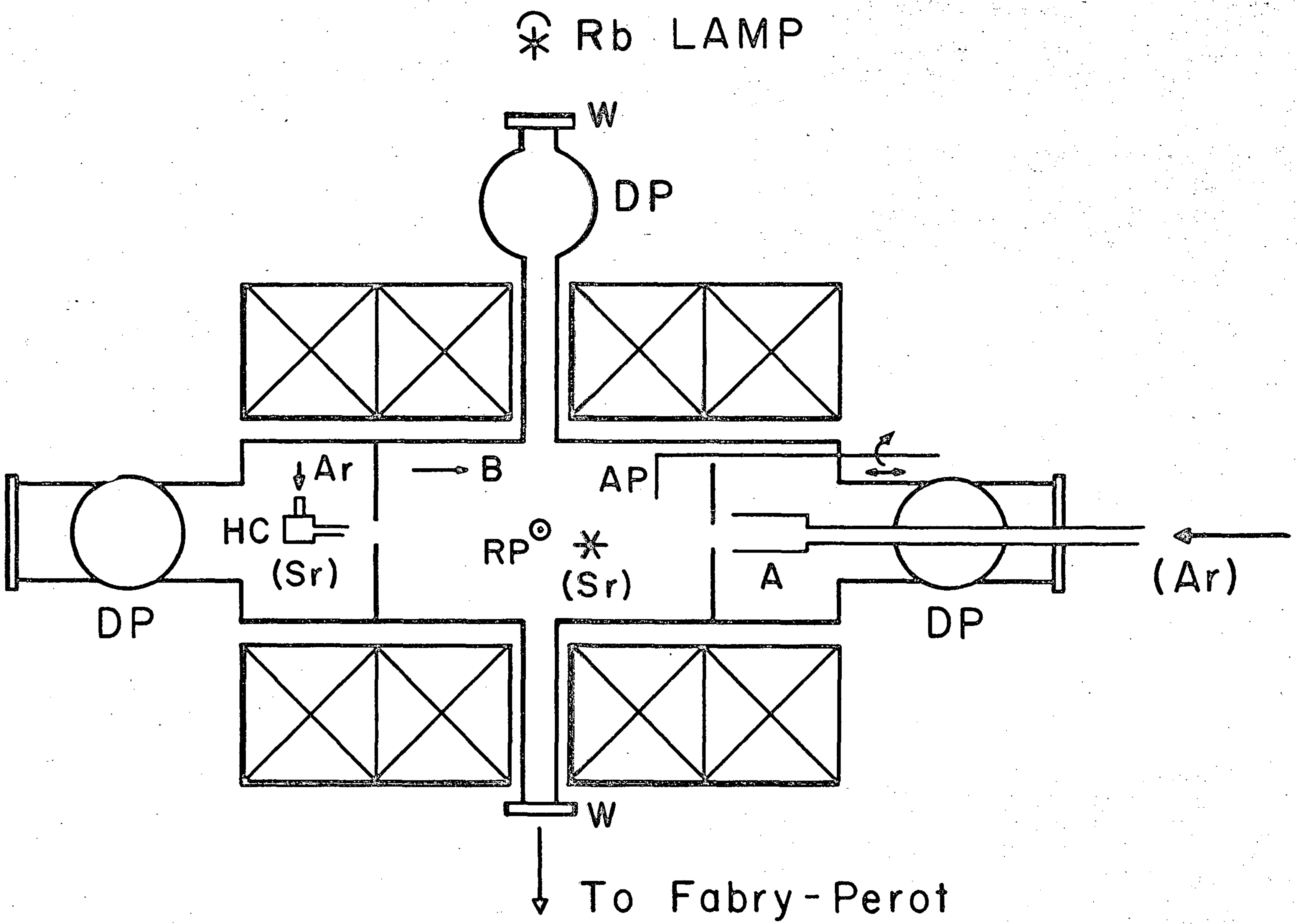

Fig. 1

MU-30689

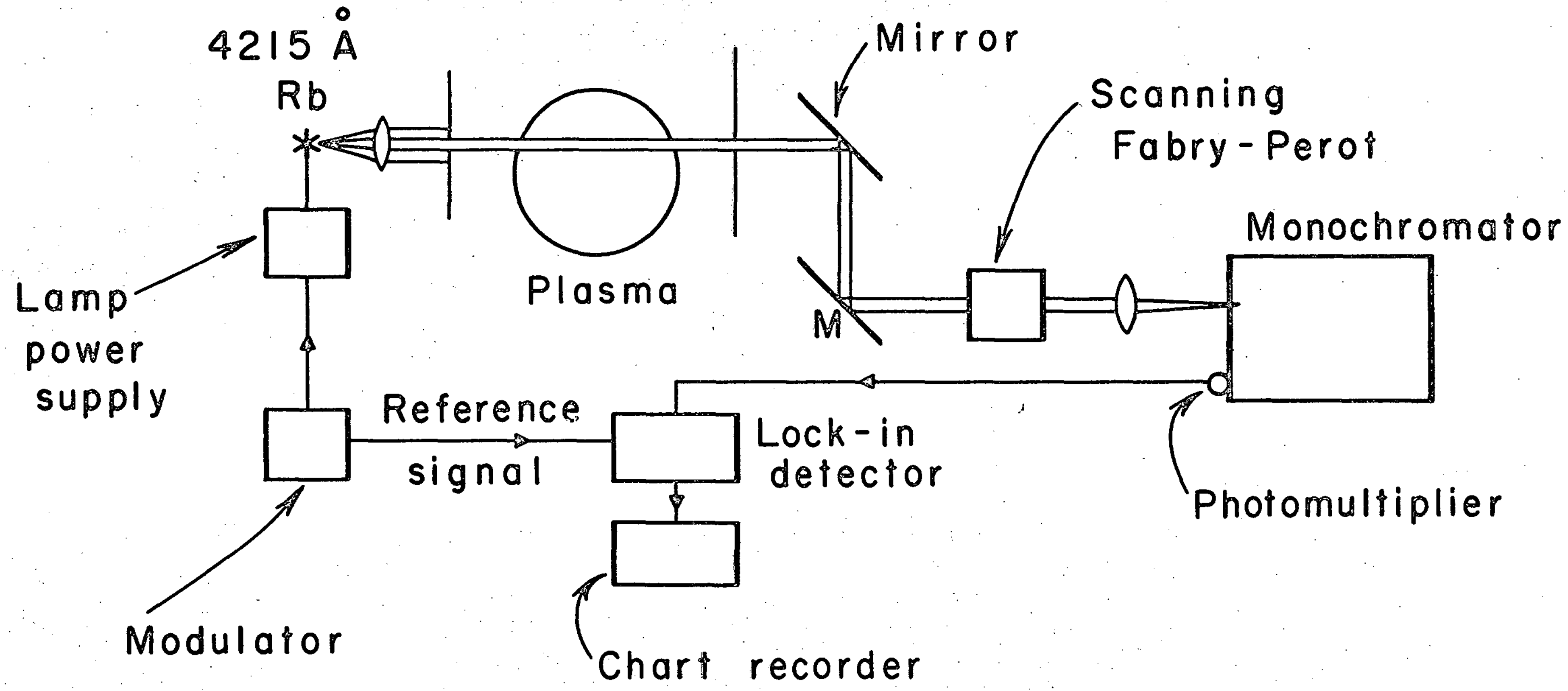

MU-30690

Fig. 2

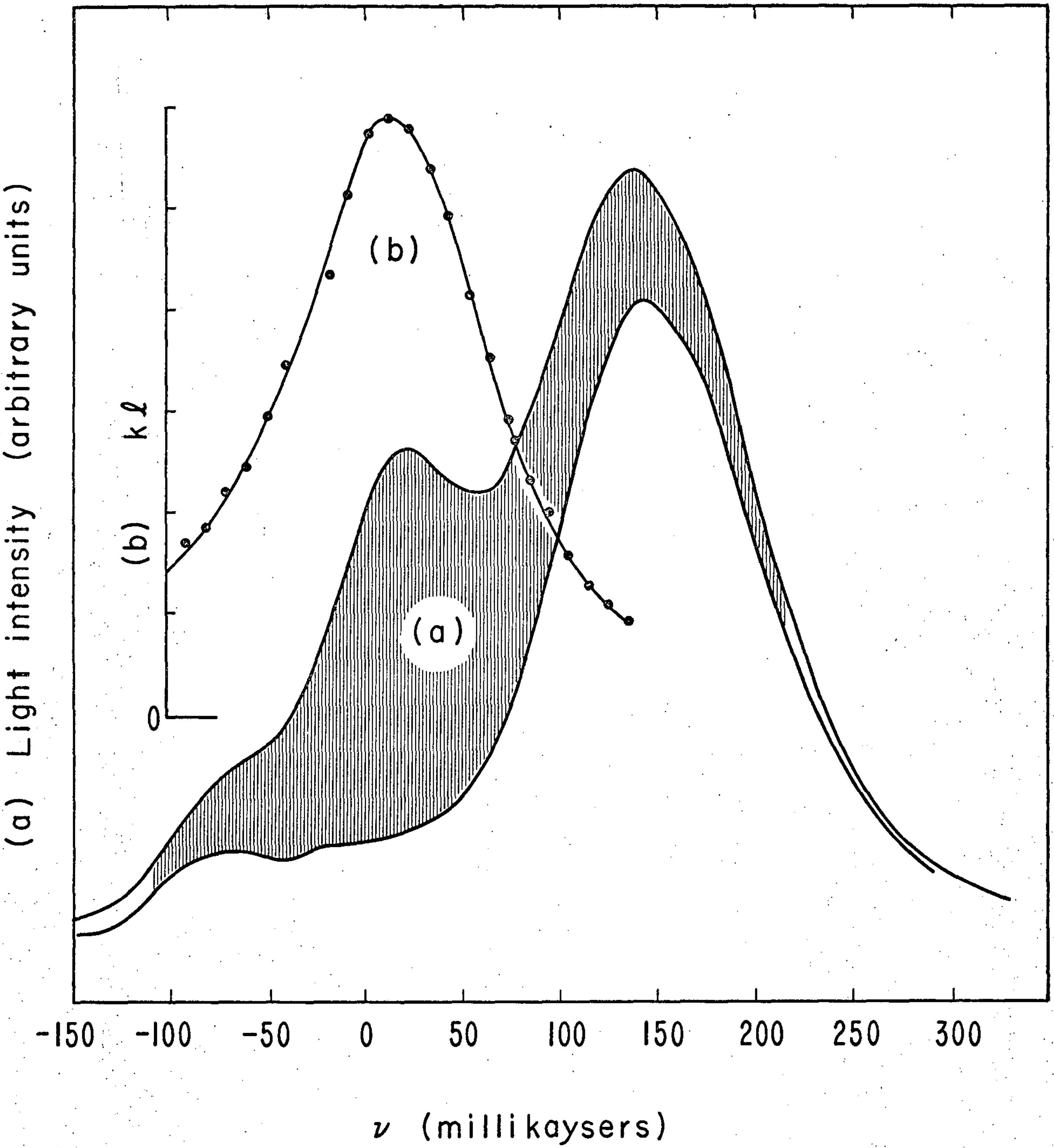

MUB-1872

Fig. 3

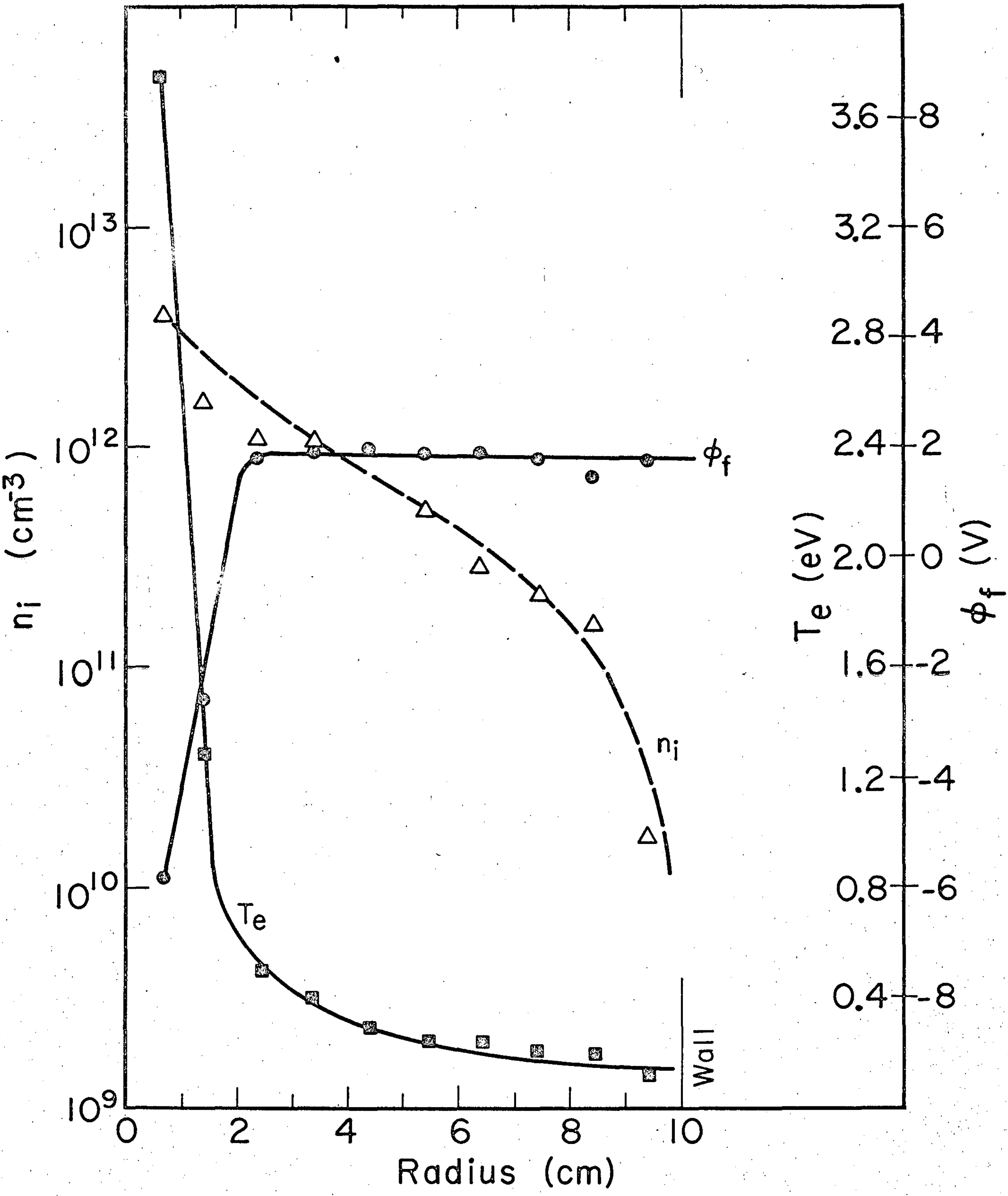

MU-30826

Fig. 4

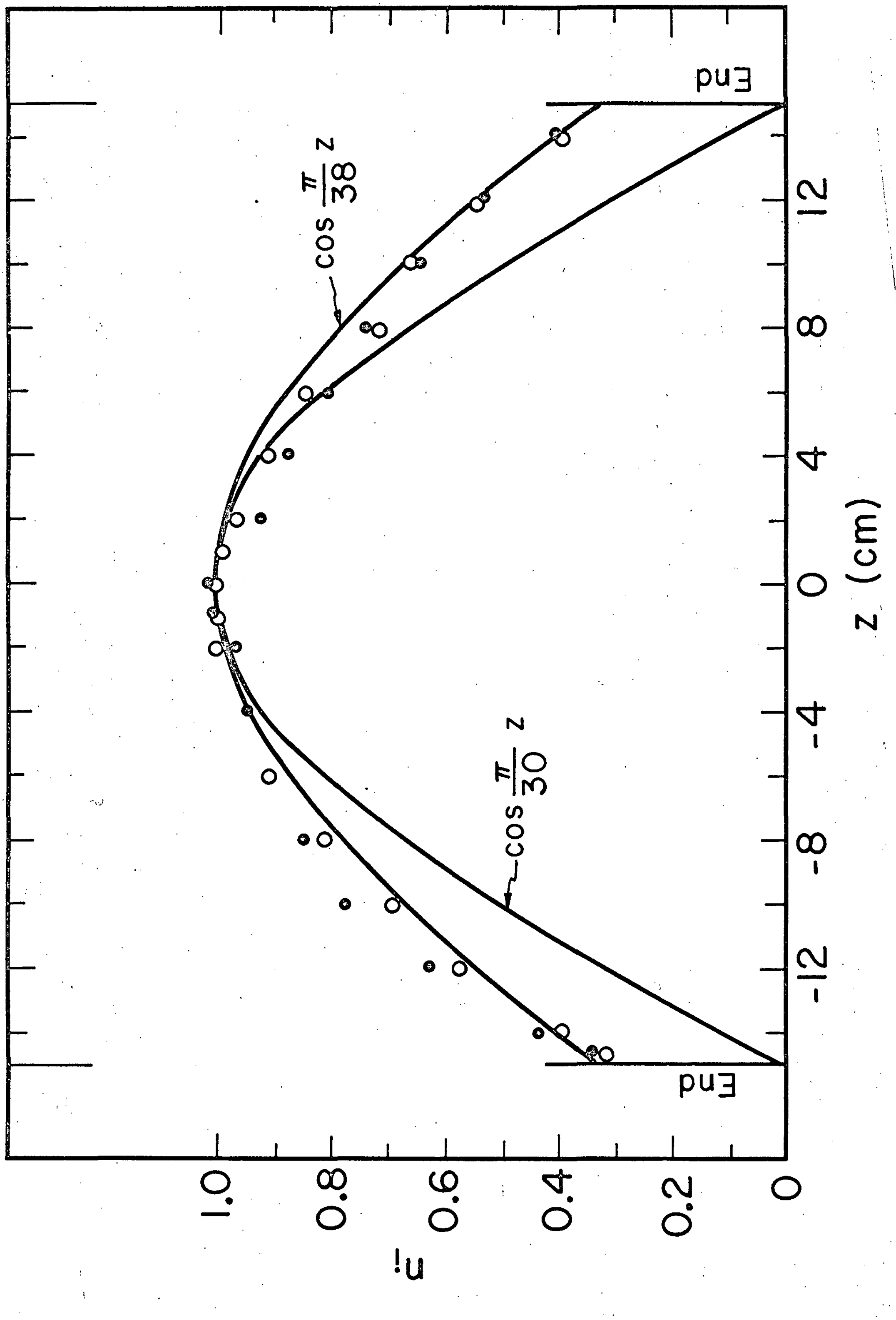

MU-30825

Fig. 5